

ANALYSIS OF FORCES INDUCED BY COATED CUTTING TOOLS AT WET AND DRY GROOVING OF HARDENED STEEL

MIROSLAV PISKA, PETRA SLIWKOVA

¹Brno University of Technology, Faculty of Mechanical Engineering, Institute of Manufacturing Technology, Brno, Czech Republic

DOI: 10.17973/MMSJ.2020_03_2019125

e-mail: piska@fme.vutbr.cz

ABSTRACT

The paper deals with a CNC grooving of hardened low-alloyed steel in flood and dry cutting conditions. A new generation of nanocomposite PVD coatings (Ti,Al)N and (Ti_{0.4},Al_{0.6})N deposited on WC-Co carbide when cutting at high cutting speed was characterized and compared. The statistical analysis of force time series acting during the machining, wear and tool life of the cutting tools have been assessed. Grooving with the coated tools and flood cooling showed to be successful and the quality of machined surface was high. The dry machining conditions were proven as disadvantageous and not recommended for any industrial practise, because the life time of the cutting tools was more than 85% shorter compared to the grooving with flood cooling.

KEYWORDS

Grooving, PVD coatings, (Ti,Al)N, (Ti_{0.4},Al_{0.6})N, cutting forces, dry machining, hardened steel.

1 INTRODUCTION

Growing requirements for a high precision machining set high demands for quality of cutting tool material. This is especially true for grooving operations – Figure 1, where width and position of a groove must be strictly precise [Fofana 2003, Jawahir 2000, Ee 2003]. To solve that problem it is necessary to consider many factors - workpiece material, cutting tool geometry, cutting conditions, wear and a use of cooling fluid. The main factor today which benefits to the life time of cutting tools is deposition of hard and wear resistant coatings [Humar 2008, Derflinger 2006, Klostermann 2005, Rech 2006, Bobzin 2017, Vijayan 2018].

In this work the new nanocomposite coatings (Ti,Al)N and (Ti_{0.4},Al_{0.6})N were tested to assess a quality of grooves in conditions of dry and wet machining of hardened steel.

2 THEORY OF THE CUTTING TEST

Forces acting during the machining – Figure 1b - provide valuable information about machining accuracy, machined surface quality, machine tool vibration, power requirements, wear and tool life [Parakkal 2001, Wanigarathne 2005]. Theoretically, resultant force F in turning operation, which includes cutting force F_c , feed force F_f and passive force F_p , could be defined from empirical expressions (1-4) [Shaw 2005, Forejt 2006]:

$$F_c = C_{Fc} \cdot a_p^{x_{Fc}} f_p^{y_{Fc}} \quad (1)$$

$$F_f = C_{Ff} \cdot a_p^{x_{Ff}} f_p^{y_{Ff}} \quad (2)$$

$$F_p = C_{Fp} \cdot a_p^{x_{Fp}} f_p^{y_{Fp}} \quad (3)$$

$$F = \sqrt{F_c^2 + F_f^2 + F_p^2}, \quad (4)$$

where C_{Fc}, C_{Ff}, C_{Fp} are material constants and x_{Fc}, x_{Ff}, x_{Fp} express the influence of axial depth of the cut and a_p , and y_{Fc}, y_{Ff}, y_{Fp} the effect of the feed on the tool force loading.

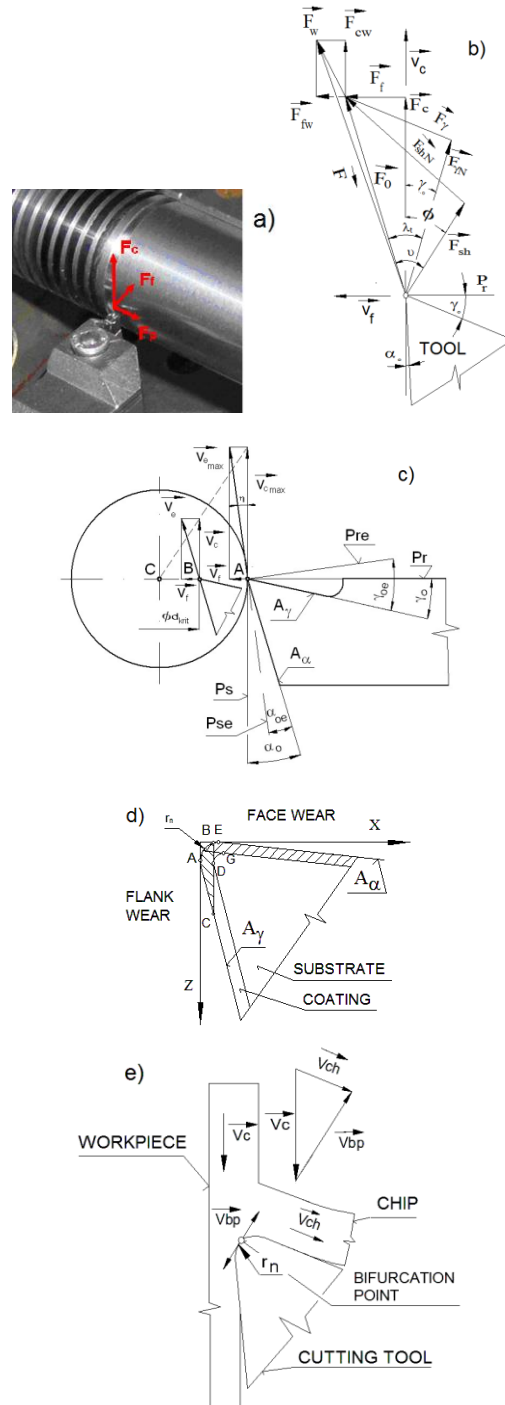


Figure 1. Grooving and cutting-off analysis. (a) An example of the tool: F_c – cutting force, F_f – feed force, $F_{\gamma N}$ – force acting perpendicularly the rake plane A_γ , F_χ – force acting along the rake A_γ , F_{shN} – force acting perpendicularly to the shear plane, F_{sh} – force acting along the rake shear plane, F_o – resultant force (without wear of tool), F – total force (regarding wear of tool), ϕ – shear angle, λ_t – Coulombian angle of friction, P_r – tool reference plane, P_{re} – working cutting edge plane, P_s –

tool cutting edge plane, P_{se} – working cutting edge plane, (b) loading of the tool and force composition regarding also wear of cutting tool, (c) the change of effective tool geometry: γ_o – tool orthogonal rake angle, γ_o – working tool orthogonal rake angle, α_o – tool orthogonal rake angle, α_{oe} – working tool orthogonal rake angle, (d) flank and face wear of the coated tool: A_{er} – flank face, (e) speed vector diagram for chip production (v_c - cutting speed, v_{ce} - effective cutting speed, v_f - feed velocity, v_{ch} - chip velocity, v_{bp} - velocity at the bifurcation point, r_n - cutting edge radius).

However, these formulations do not include the effect of wear as a function of cutting time, so it should be modified into the equations (5–8):

$$F_c = F_{c0} + F_{cw} \quad (5)$$

$$F_{c0} = A_D \cdot k_c = a_0 \quad (6)$$

$$F_{cw} = a_1 \cdot t + a_2 t^2 \quad (7)$$

$$F_c = a_0 + a_1 \cdot t + a_2 t^2 \quad (8)$$

Where F_{c0} represents the cutting force for a sharp cutting edge and F_{cw} includes the effect of wear on the cutting force. According to our experimental work, polynomial functions reflect the wear phenomena very relevantly for all measured components in the cutting time as a common function. The other components can be simplified in the following forms (9–10).

$$F_f = k_{ff}(t) \cdot F_c \quad (9)$$

$$F_p = k_{fp}(t) \cdot F_c \quad (10)$$

The magnitude of the resultant force was the same for the both theoretical variations.

A typical problem linked to the grooving is the change of cutting speed according to the cut diameter when machining with the constant number of rotation – Figure 1c. The effective geometry of tool changes and a critical diameter when effective flank angle is zero can be predictive. In that moment cutting tool can be overloaded and broken.

A special attention should be paid to the coated tools where wear developments passes through the coatings and when the substrate is revealed. The mechanics of the wear is affected by the changes in momenta and inertia at the interface when chip is produced – Figure 1e.

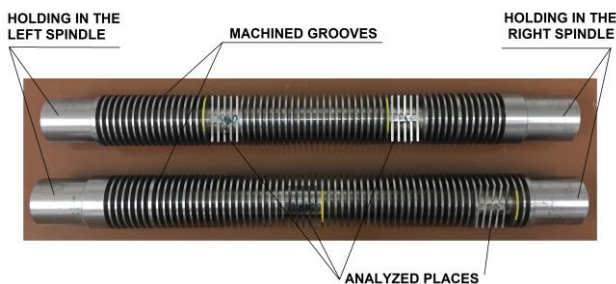


Figure 2. Examples of the workpieces and analyzed places.

3 EXPERIMENTAL PROCEDURE

The material of a workpiece was hot rolled steel DIN 50 CrV4 with tensile strength R_m 885–1,030 MPa, hardened to 30 ± 1 HRC. In total, 45 bars have been tested, each $\varnothing 38/380$ mm – Figure 2. The width of a groove was 3 ± 0.05 mm, depth of grooves 9.5 mm, pitch of grooves 4.5 mm. Chemical composition of the material is listed in Table 1. Structure of the material was created by tempered martensite, carbides and fine dispersion of secondary carbides, residual austenite, oxides and MnS inclusions – Figure 3. Machining of a workpiece was

carried out in wet and dry cooling conditions as short time cutting tests. The Kistler® 9257B dynamometer and charge amplifiers Kistler® 9011A, fully controlled by PC, were used for cutting force measurements, fixed to the lathe SU50 2A.

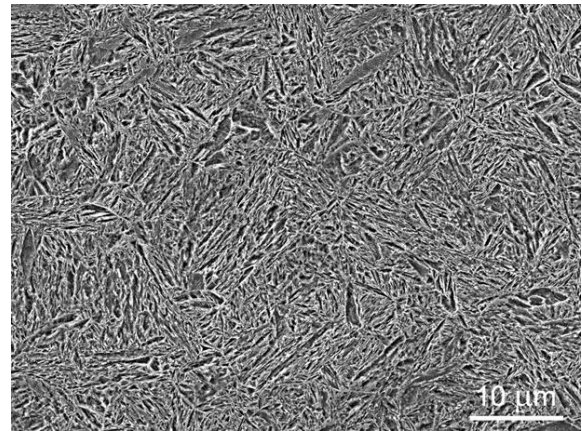


Figure 3. Structure of the machined material (martensite, carbides). Nitral 2%.

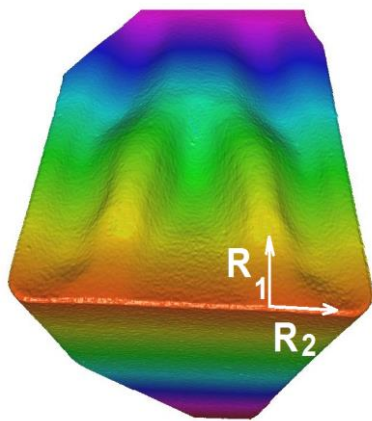
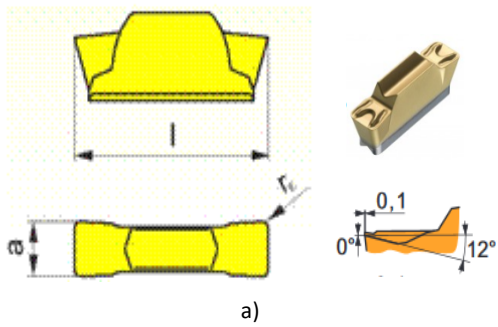
Steel	Chemical composition [weight %]				
DIN50CrV4	C	Mn	Si	Cr	V
	0.47–0.55	0.70–1.00	0.15–0.40	0.90–1.20	0.10–0.20
	Ni	P	S	Fe	
	0.30 max.	0.035 max.	0.035 max.	rest	

Table 1. Workpiece material (Mn-Cr-V hardened steel)

Cutting inserts LCMF 031602-F; grade HF10 (Dormer Pramet®) – Figure 4 - were used for the grooving, clamped to the tool holder ISO GFIR/L 1616 H 03 – Figure 3b. The cemented carbide was made from WC+Co (90% W), grain size 2-4 µm. The geometry of the cutting inserts is shown in the Figure 4a,c where the parameters are: $a = 3 \pm 0.05$ mm, $l = 16.4$ mm, $r_\epsilon = 0.2$ mm. Roughness of the rake face measured along and perpendicularly to the main cutting edge in terms of R_a (arithmetic average of the roughness profile), R_q (root mean square deviation) and R_z (average maximum height of assessed profile) was very good – see Figure 4c, as well as the cutting edge radius (about 30 µm).

Trademark of coating, group, composition coating structure	Hardness HV 0.05 [MPa]	Maximal working temperature [°C]	Coefficient of friction [-]
Tinalox® Supernitrid (Ti,Al)N Nanocomposite	3,500	1,000	0.3
Hyperlox® Supernitrid (Ti _{0.4} ,Al _{0.6})N Nanocomposite	3,700	1,100	0.3

Table 2. Nominal physical properties of the tested PVD coatings



R_1 : Ra: 0.754 μm
 Rq: 0.930 μm
 Rz: 3.881 μm

R_2 : Ra: 1.034 μm
 Rq: 1.441 μm
 Rz: 6.790 μm

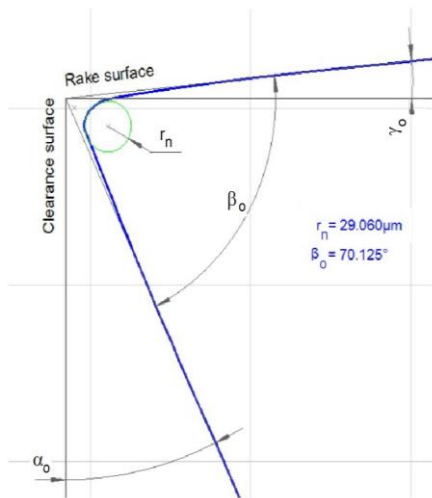


Figure 4. Cutting tool: a) the insert geometry; b) the tool holder; c) the microgeometry of the edge

New nanocomposite PVD coatings (Ti,Al)N and (Ti_{0.4},Al_{0.6})N - Table 2 - were deposited on the substrates by means of a magnetron sputtering technology by CemeCon® with CC800/9ML system use. The temperature of inserts during the coating deposition process was between 450÷480°C, thickness of the deposited coatings was 6±1 μm (proved by the ball-erosion Kalo-test, see Figure 5). In general, these coatings remain normally stable in the single-phase cubic structure used for metal working applications up to more than 800°C [Bobzin 2017, Vijayan 2018].

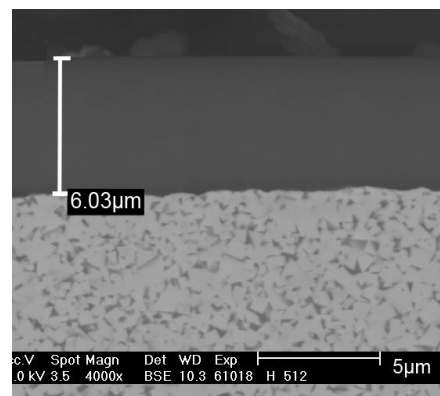
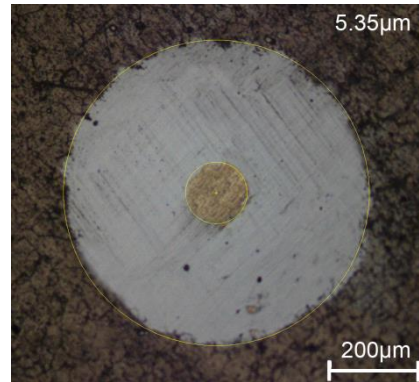


Figure 5. Analyses of the coatings: a) Kalo-test of (Ti,Al)N coating; b) (Ti_{0.4},Al_{0.6})N coating structure (BSE)

Morphologies of the coatings surfaces were studied with the use of scanning electron microscope microscope XL 30 Philips® working in SE and BSE regimes. The PVD coatings (Ti,Al)N and (Ti_{0.4},Al_{0.6})N had a very fine, pore free structure and uniform interface, which was beneficial to adhesion – Figure 5. Both types of coatings had an increased hardness compared to standard (Ti,Al)N coatings as well as superior stability. It was due to their nanocomposite structure where crystals of (Al,Ti)N (enriched with Al) were embedded into matrix (Ti,Al)N (enriched with Ti). The cutting tests were performed on the CNC lathe Kovosvit MAS® SP 280 SY with Sinumerik 840D CNC. The workpieces were clamped with the main spindle chuck and a counter spindle chuck, so a very rigid and stabilized blank holding was realized. For the wet machining a cooling fluid ECOCOL 68 CF2, Fuchs Oil Corporation®, was applied. Cooling fluid volume concentration in water was 5-6%, pressure 60 bars, fluid flow was about 0.2-0.3 liter per second. The cutting conditions and some results of the cutting tests can be seen in Figure 5. The statistical assessment was done in Minitab® 18, Pennsylvania, USA.

4 RESULTS

Wear of the tested inserts had a gradual degradation behavior, with different intensiveness for the wet and dry cutting – Figure 6. During the dry grooving operation a high noise, sparkles, bad chip formation, high energy consumption, etc. were observed. Moreover, values of the cutting forces have grown considerably in comparison to wet machining, due to rake and flank wear of inserts. Values of forces acting during the wet machining are shown in Table 3 and Figure 7. The results for passive forces F_p were affected by slight chattering of the workpiece and a significantly lower rigidity of the slim tool holder in the axial direction compared to the tangential orientation. Nevertheless, all coefficients for the tool loading analyses are given in the Table 4 and Figure 8. According to the statistic assessment, the medians of total cutting forces for worn inserts with PVD (Ti,Al)N and (Ti_{0.4},Al_{0.6})N coatings were not equal, ($p=0.05$) – Figure 9.

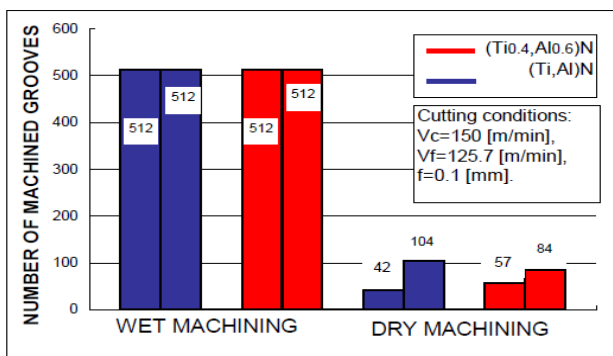


Figure 6. Cutting performance of the coated tools

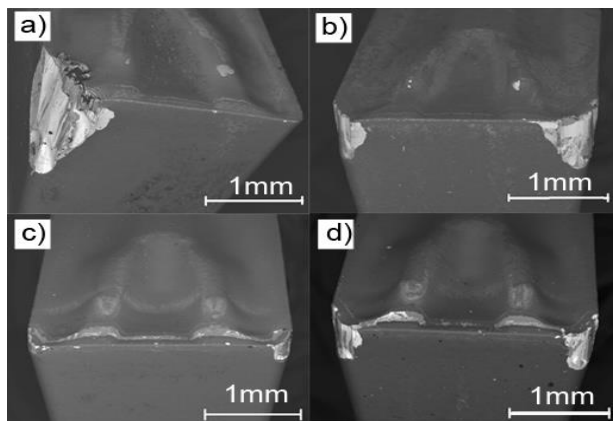


Figure 7. Abrasive wear of the cutting inserts in dry conditions - a)(Ti,Al)N, b)(Ti_{0.4},Al_{0.6})N, and wet conditions - c)(Ti,Al)N, d)(Ti_{0.4},Al_{0.6})N

Force	(Ti _{0.4} ,Al _{0.6})N Hyperlox®		
	Machining time t [min]		
	0.08	18.99	42.66
F_c [N]	874.88 ±116.34	934.43 ±116.34	874.88 ±116.34
F_f [N]	394.17 ±97.99	485.40 ±97.99	394.17 ±97.99
F_p [N]	1.93 ±46.21	5.44 ±46.21	1.93 ±46.21
Force	(Ti,Al)N Tinalox®		
	Machining time t [min]		
	0.08	18.99	42.66
F_c [N]	895.24 ±125.38	954.95 ±125.38	1186.00 ±125.38
F_f [N]	350.57 ±99.32	453.31 ±99.32	592.94 ±99.32
F_p [N]	1.05 ±42.12	7.05 ±42.12	93.23 ±42.12

Table 3. An overview of the measured forces (means, standard deviations)

	(Ti _{0.4} ,Al _{0.6})N Hyperlox®				
	F _c	F _f	F _p	K _{Ff}	K _{Fp}
a₀	874	393.83	1.900	0.450	0,002
a₁	0.556	4.210	0.372	0.005	4.10 ⁻⁴
a₂	0.136	0.032	-0.010	-6.10 ⁻⁵	1.10 ⁻⁵
	(Ti,Al)N Tinalox®				
	F _c	F _f	F _p	K _{Ff}	K _{Fp}
F_c [N]	895.22	350.15	1.143	0.388	-0.001
F_f [N]	0.200	5.224	-1.171	7.10 ⁻³	-7.10 ⁻⁴
F_p [N]	0.155	0.011	0.078	-1.10 ⁻⁵	6.10 ⁻⁵

Table 4. Table of the statistical (regression) constant for all measured forces

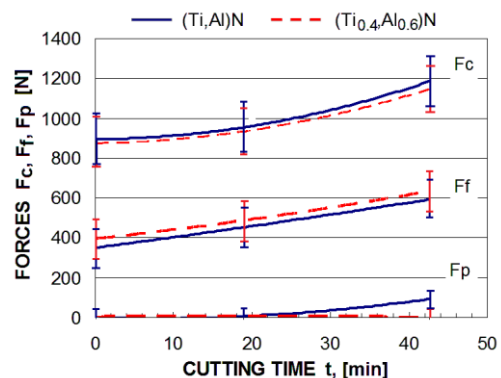


Figure 8. Time series of forces (mean values, standard deviations)

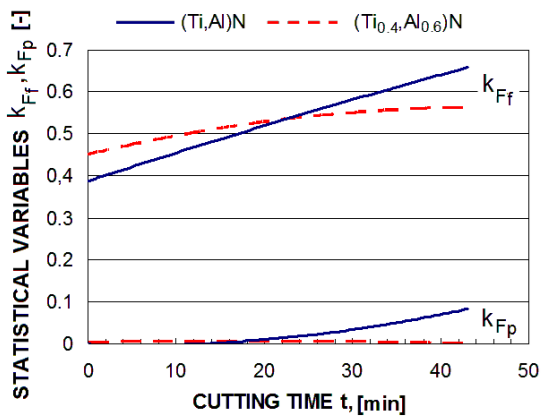


Figure 9. Time series of statistical (regression) constants

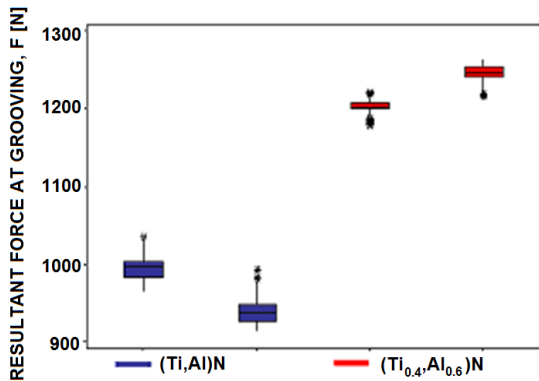


Figure 10. Comparison of the resultant forces at grooving for the tested inserts

Quality of the machined surface in terms of average roughness (Ra) was assessed with Form Talysurf Ultra 50, Taylor Hobson Precision® and Alicona IF G5 after cutting the samples. Three kinds of surfaces have been analyzed - Figure 11 - in the terms of roughness. The quality of side surfaces - left - marked as Ra(L) and right Ra(R), that were better in comparison to the front Ra(F) (by 15-20%) – Figure 12,13. No significant difference between Ra(L) and Ra(R) was found ($p=0.05$) for most measurements. Average roughness values were showed increasing values with a number of the machined grooves – Figure 14. This process had a systematic behaviour with a normal data distribution, ($p=0.05$).

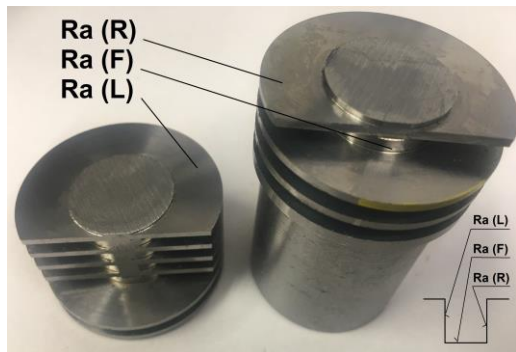


Figure 11. An example of samples for the surface analyses, positions of measurements

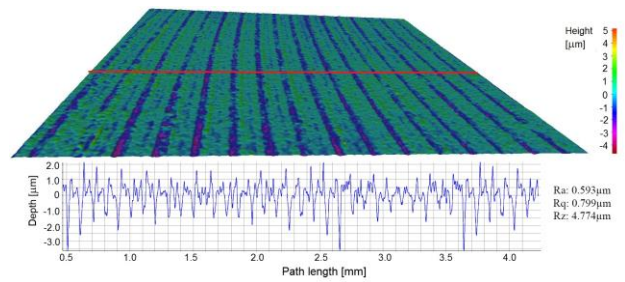


Figure 12. An example of the machined surface on the left side of the groove Ra(L)

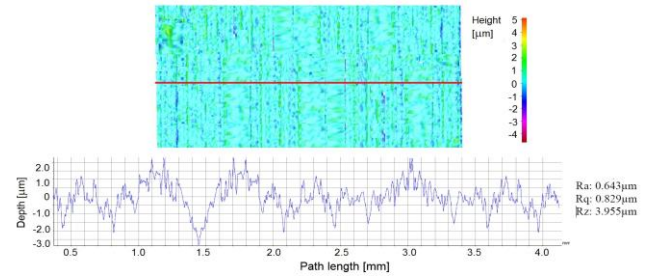


Figure 13. An example of the machined surface on the front side of the groove Ra(F)

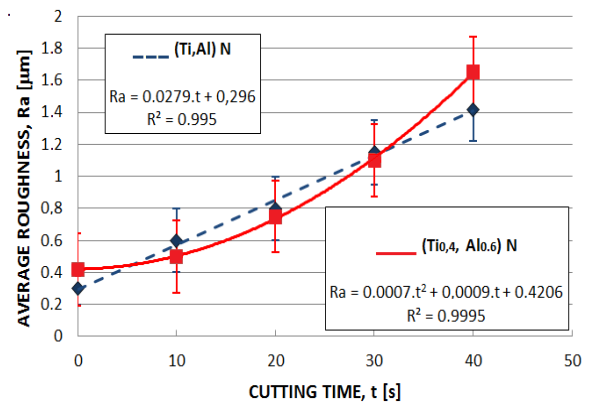


Figure 14. The average roughness of the machined side groove surfaces (the parameter R^2 reflects the level of statistical correlation)

5 DISCUSSION

The low cutting performance of the coated tested inserts without cooling was surprising compared to our previous research works. However, if the high mechanical properties of the machined material, dry cutting conditions and the fact that the coatings work as a good thermal insulation barrier preventing the heat flux into the slim cutting tool, then a simplified calculation for the heat generation and prevailing distribution into chip can be written as:

$$F_c \cdot v_c \cdot t = m \cdot c_p \cdot \Delta T, \quad (6)$$

in which apart the already mentioned symbols t is the time for cutting, m is mass of material converted into chip, c_p is specific heat capacity, and ΔT is the temperature rise of the chip (all other sources and ways of distributions are neglected). So the mass of produced chip via plastic deformation m can be rewritten according the un-deformed chip cross section Ad as

function of the feed per rotation f , axial width of cut a_e , specific mass density and specific cutting condition

$$m = A_D \cdot v_c \cdot \rho \cdot t = f \cdot a_e \cdot v_c \cdot \rho \cdot t \quad (7)$$

and after a simplification the expected temperature rise can be predicted as

$$\Delta T = \frac{F_c}{f \cdot a_e \cdot \rho \cdot c_p} \quad (8)$$

Taking into consideration the real cutting conditions ($v_c=150$ m/min, $f=0.1$ mm, $a_e=3$ mm), mass per unit volume ($\rho =7800$ kg.m⁻³), specific heat capacity ($c_p =460$ J kg⁻¹ K⁻¹) and measured values of F_c (900 N approximately for the sharp cutting edge), then the temperature rise is much bigger (more than 800°C) then the temperatures of the coating deposition process (450÷480°C). However, for the referred limited working temperatures (1,000°C) the needed cutting force should be about 1,000 N. The measured values of the cutting force in the end of life reached 1,200 N, so the flood cooling is really necessary and calculated value of the cooling intensity for the machine and cutting process more than 1 kw. The roughness parameters measured with both devices showed very similar results (due to matt machined surfaces).

6 CONCLUSIONS

Several conclusions from the research work can be made:

- excellent cutting performances of the PVD coated tools when grooving were proved experimentally, however, the effective flood cooling is needed;
- the life time of the cutting tools was for 85% longer compared to dry machining, and exceeded 25 minutes of machining at the cutting speed of 150 m/min and feed per rotation 0.1 mm for the tempered martensitic steel;
- lower average values of the total forces were found during the wet machining – for both types of coatings the reduction was 250 N approximately, with lower values of their variances also (30%);
- no continual chip formation was observed in dry machining, but rather poor material forming was observed, accompanied with formation of macro-particles, high noise, tendency to chattering and rapid tool wear or insert fracture;
- a statistically significant difference between medians of the total cutting forces for inserts with PVD (Ti,Al)N and (Ti_{0.4},Al_{0.6})N coatings was found ($p=0.05$);
- no statistically significant difference was confirmed for average arithmetical profile deviations ($p=0.05$) of machined surfaces for the tested coatings ((Ti_{0.4},Al_{0.6})N, (Ti,Al)N).

ACKNOWLEDGEMENTS

This research work was supported by the FME BUT Brno, Czech Republic as the "Research of perspective production technologies", FSI-S-19-6014 and Ministry of Industry and Trade, project "Application of the New Surface Treatment Technologies in Metal Packaging Industry", FV40313.

REFERENCES

- [Bobzin 2017] Bobzin, K. High-performance coatings for cutting tools. CIRP Journal of Manufacturing Science and Technology. 2017; 18:1-9.
- [Derflinger 2006] Derflinger, V. H., Schutze, A. and Ante, M. Mechanical and structural properties of various

alloyed TiAlN-based hard coatings. Surface & Coatings Technology, 2006, Vol. 200, pp. 4693 – 4700.

- [Ee 2003] Ee, K.C., Balaji, A.K. and Jawahir, I.S. Progressive Tool-wear Mechanisms and their Effects on Chip Curl/Chip-form in Machining with Grooved Tools. Wear, 2003, Vol. 255, pp. 1404-1413.
- [Fofana 2003] Fofana, M.S., Ee, K.C. and Jawahir I.S., Machining Stability in Turning Operations when Cutting with a Progressively Worn Tool Insert. Wear, 2003, Vol. 255, pp. 1395-1403.
- [Forejt 2006] Forejt, M., Piska, M. Theory of Machining, Forming and Cutting tools. Brno: CERM, 2006. ISBN 80-214-2374-9
- [Humar 2008] Humar, A. Materials For Cutting Tools. Prague: MM publishing, 2008. ISBN 978-80-254-2250-2
- [Jawahir 2000] Jawahir, I. S. and Balaji, A. K. Predictive Modeling and Optimization of Turning Operations with Complex Grooved Tools for Curled Chip Formation and Chip Breaking. Machining Science & Technology, 2000, Vol. 4, pp. 399-443.
- [Klostermann 2005] Klostermann, H., Bfcher, B., Fietzke, F., Modes, T. and Zywitzki, O. Nanocomposite oxide and nitride hard coatings produced by pulse magnetron sputtering. Surface & Coatings Technology, 2005, Vol. 200, pp. 760– 764.
- [Parakkal 2001] Parakkal, G., Zhu, R., Kapoor, S. G. and DeVor, R. E. Modeling of turning process cutting forces for grooved tools. International Journal of Machine Tools & Manufacture, 2002, Vol. 42, pp.179-19.
- [Rech 2006] Rech, J. Influence of cutting tool coatings on the tribological phenomena at the tool–chip interface in orthogonal dry turning. Surface & Coatings Technology, 2006, Vol. 200, pp. 5132 – 5139.
- [Shaw 2005] Shaw, M. C. Metal Cutting Principles. New York: Oxford University Press, 2005. ISBN 0-19-514206-3
- [Vijayan 2018] Vijayan, D., Manoj Kumar, Y.G. A Preliminary Investigations on Second Generation Nano Composite Super Nitride Coatings on Astm A681 Tool Steels. 3rd International Conference on Materials and Manufacturing Engineering 2018, IOP Conf. Series: Materials Science and Engineering 390 (2018) 012054; Kanchipuram, Tamilnadu; India; 8.-9.3.2018; doi:10.1088/1757-899X/390/1/012054
- [Wanigarathne 2005] Wanigarathne, P.C., Kardekar, A.D., Dillon, O. W., Poulachon, G. and Jawahir, I.S. Progressive Tool-wear in Machining with Coated Grooved Tools and Its Correlation with Cutting Temperature, Wear, 2005, Vol. 259, pp. 1215-1224.

CONTACTS:

Prof. Ing. Miroslav Piska, CSC.
Brno BUT, Faculty of Mechanical Engineering,
Institute of Manufacturing Technology,
Technicka 2, 616 69 Brno, Czech Republic
tel.: +420 5 4114 2555, e-mail: piska@fme.vutbr.cz